# Clustering Dynamics in Water/Methanol Mixtures: A Nuclear Magnetic Resonance Study at 205 K < *T* < 295 K

**Carmelo Corsaro,*,† Jeroen Spooren,† Caterina Branca,† Nancy Leone,† Matteo Broccio,†,‡ Chansoo Kim,§ Sow-Hsin Chen,§ H. Eugene Stanley,|| and Francesco Mallamace†,§**

*Dipartimento di Fisica and CNISM, Università di Messina, C. da Papardo, S. ta Sperone 31, 98166 Messina, Italy, Department of Physics, Carnegie Mellon University, 5000 Forbes Avenue, Pittsburgh, Pennsylvania 15213, Department of Nuclear Science and Engineering, Massachusetts Institute of Technology, Cambridge, Massachusetts 02139, and Center for Polymer Studies and Department of Physics, Boston University, Boston, Massachusetts 02215*

*Received: April 21, 2008; Revised Manuscript Received: June 10, 2008*

Proton nuclear magnetic resonance ($^1$H NMR) experiments have been performed to measure the spin−lattice, $T_1$, and spin−spin, $T_2$, relaxation times of the three functional groups in water/methanol mixtures at different methanol molar fractions ($X_{MeOH}$ = 0, 0.04, 0.1, 0.24, 0.5, 1) as a function of temperature in the range 205 K < *T* < 295 K. The measured relaxation times in the mixtures, at all the methanol molar fractions, are faster than those of pure water and methanol because of strong interactions, resulting in a complex hydrogen bonding dynamics that determines their thermodynamic properties. In particular, we observe how the interplay between hydrophobicity and hydrophilicity changes with temperature and influences the peculiar thermal behavior of the NMR relaxation times of the solution. The obtained results are interpreted in terms of the existence of stable water−methanol clusters at high temperature whereas, upon cooling to low temperature, clusters of single species are present in the mixture.

## Introduction

Water is the most abundant liquid on Earth and plays a key role in all biological systems. Notwithstanding liquid water has been up to date widely investigated, its peculiar properties are still not fully understood. Water anomalies are more pronounced in the supercooled regime, where its thermodynamic response functions, e.g., the isobaric specific heat and the isothermal compressibility, increase rapidly with decreasing temperature.[1] There are two thermodynamically consistent hypotheses which attempt to explain water anomalies: the singularity free scenario,[2] in which the experimentally observed increases in water response functions upon supercooling are explained as the consequence of the existence of a negative sloped line of temperatures of maximum density in the (*T*, *P*) plane; the liquid−liquid critical point (LLCP) hypothesis[3] predicts a phase transition between a low-density (LDL), low *T* and *P*, and a high-density (HDL) liquid phase, high *T* and *P*. In the LDL phase, an open and localized hydrogen bonded (HB) network exists, similar to that in ice. Contrarily, the HB network in the HDL phase does not develop extensively. The liquid−liquid transition line terminates in the predicted second critical point of water from which the so-called *Widom Line* (WL), the critical isochore, locus of correlation length maxima, initiates.[4] This last hypothesis has been receiving support from both experiments and computer simulations.[4–12]

Recent experiments, performed on protein (lysozyme) hydration water,[13] have indicated that the dynamic behavior associated with the protein glass transition can be ascribed to the crossing of the WL of the bound water. This was also confirmed by computer simulations on the same system.[13,14]

Although all these studies show unambiguously that the protein glass transition is connected to the change of local hydrogen bond patterns of hydration water, the underlying microscopic mechanisms are still to be unveiled.

A protein possesses amphiphilic groups: the hydrophobic moieties repel water molecules and the hydrophilic ones attract them, hence a complex HB network is generated. The observation of a biological inactivity for anhydrous proteins, as well as the coincidence of the activation temperature of hydrated proteins with the WL of water,[13,14] lead to the conclusion that an insight into the interactions between the amphiphilic groups and water is fundamental to the comprehension of biological phenomena.

In this frame, aqueous solutions of small amphiphilic molecules can be used as model systems to understand such interactions. The simplest amphiphilic molecule is methanol, with the chemical formula $CH_3OH$, which consists of a single hydrophilic (OH) and a single hydrophobic ($CH_3$) group. Methanol in aqueous media has also several important industrial applications such as the production of hydrogen gas for fuel cells.[15]

Although water and methanol are relatively simple molecules, it is well-known that the thermodynamic and transport properties of their mixtures show an anomalous behavior with respect to those expected from an ideal mixture of the pure liquids. For example, in the mixture the diffusion coefficient and the excess entropy are considerably smaller, and the viscosity notably larger (see Table 1),[16–18] indicating strong interactions between these two liquids.

Understanding anomalies of this system have been the subject of numerous analyses, one of the earliest being that by Frank and Evans who proposed a structural origin of its behavior.[19]

* To whom correspondence should be addressed. E-mail: ccorsaro@unime.it.
† Università di Messina.
‡ Massachusetts Institute of Technology.
§ Carnegie Mellon University.
|| Boston University.

10.1021/jp803456p CCC: $40.75 
Published on Web 08/02/2008

**TABLE 1: Studied Methanol Molar Fractions, Their Relative Methanol/Water Molecular Ratio,[a] Equilibrium Melting Temperatures, and Viscosities at 298 K**

| molar fraction ($X_{MeOH}$) | $n_{MeOH}/n_{H_2O}$ | $T_m$ (K) [b] | $\eta$ (cP)[c] |
|---|---|---|---|
| 0 | 0/1 | 273 | 0.89 |
| 0.04 | 1/25 | 269 | 1.06 |
| 0.10 | 1/9 | 261 | 1.31 |
| 0.24 | 1/3 | 240 | 1.58 |
| 0.50 | 1/1 | 196 | 1.33 |
| 1 | 1/0 | 176 | 0.54 |

[a] The molecular ratio gives the number of water molecules per molecule of methanol present in solution. [b] Reference 34. [c] Reference 18.

In particular, they speculated that the normal water structure is significantly enhanced by the hydrophobic entity, resulting in a more ordered structure near the methyl headgroup, interpretable as an "iceberg-like" structure. It is reasonable thinking that water at a hydrophobic surface loses hydrogen bonds, so its enthalpy increases. In order to compensate for the rise in enthalpy, in proximity of a hydrophobic site, the local arrangement of water molecules expands to form low-density water clusters with a resulting lower entropy.[19] Also, the folding of proteins is believed to be principally induced by the entropy loss of water molecules around their hydrophobic sites.[20]

However, further studies on these systems yielded contradictory results about the enhancement of the structure of water near the hydrophobic headgroups of methanol.[17,21–28] One of the most recent analyses has reported a series of neutron diffraction studies which show that at low alcohol concentration, a slight compressive effect is exerted on the water structure by the methanol molecules. In the opposite case (high alcohol concentration), a segregation on molecular scale takes place in which the methyl groups are pushed toward each other and the methanol hydroxyl groups organize themselves around small water clusters.[17,21–24] molecular dynamics simulations have confirmed that water and methanol in solution are not randomly mixed, but form clusters.[24,26] In a particular concentration range, these clusters seem to increase in size and percolate, even if their structures break and reform very rapidly (on the order of picoseconds, ps).[21] This could imply that the peculiar behavior of water/methanol solutions is dynamical in origin, as asserted in ref 29. These authors, by means of depolarized Rayleigh light scattering, have studied the HB relaxation time as a function of temperature and methanol molar fraction and have ascribed the thermodynamic anomalies of the water/methanol mixture to a complex HB dynamics (occurring on the ps time scale).

In this paper we present a proton nuclear magnetic resonance ($^1$H NMR) investigation on the relaxation dynamics of methanol aqueous solutions. In particular, the longitudinal spin−lattice relaxation times, $T_1$, and the transverse spin−spin relaxation times, $T_2$, of the observed protons as a function of temperature at different concentrations were investigated. $T_1$ is related to the dipolar interactions of the observed protons with their surrounding whereas $T_2$ between protons belonging to the same species. Thus, these quantities give information about the different interactions that take place within the system. In water/methanol mixtures, hydrogen bonding is the principal source of interactions between hydroxyl groups hence by measuring $T_1$ and $T_2$ one can get a macroscopic insight of the HB dynamics. By means of high resolution $^1$H NMR spectroscopy, it is possible to study separately all the hydrogens belonging to the different functional groups present in the mixture. $^1$H NMR, as a well-known powerful method for the investigation of molecular motions and interactions, has been applied in the past to studies of both pure water and pure methanol.[30–33] Nevertheless, up to now, this technique has been scarcely employed in the study of mixtures of the two liquids, especially at low temperatures.

The aim of this work is to achieve a better understanding of the mechanisms underlying the unusual properties of the water/methanol mixture, and in particular, to determine how the interplay between hydrophobicity and hydrophilicity changes with temperature and influences the thermal behavior of the NMR relaxation times of the solution.

## Experimental Details

The NMR dynamic properties of water/methanol solutions with different methanol molar fractions ($X_{MeOH} = 0$, 0.04, 0.1, 0.24, 0.5, 1) were measured at atmospheric pressure and at different temperatures by using a Bruker Avance spectrometer, operating at the 700 MHz $^1$H resonance frequency. In particular, we have measured the proton spin−lattice and proton spin−spin relaxation times, $T_1$ and $T_2$ respectively, for the three functional groups present in solution: water hydroxyl ($OH_w$), methanol methyl ($CH_3$), and methanol hydroxyl ($OH_m$).

The sample temperature was controlled by a cold nitrogen flow and a heating element, calibrated against the standard methanol reference (4% $CH_3OH$ in $CD_3OD$) with an accuracy of 0.2 K. The investigated temperatures ranged from 295 K down to either 205 K or until solidification of the water/methanol solution.

Solvents used were ultra gradient pure water and super purity methanol both supplied by *Romil pure chemistry*. Table 1 lists the molecular ratios, the equilibrium melting temperatures ($T_m$)[34] and the viscosities[18] at 298 K corresponding to the investigated $X_{MeOH}$.

In an NMR experiment, the system is immersed in a static and homogeneous magnetic field which induces the macroscopic magnetization (the vector sum of all the active nuclear spins) to align with respect to the field direction. In order to measure the relaxation time constants of the investigated system, this has to be perturbed with an appropriate pulse sequence; i.e. a sequence of radio frequency pulses, applied in the plane orthogonal to the field direction. Each pulse tilts the magnetization vector by an angle (with respect to the static field direction) whose amplitude depends on the pulses power, duration and repetition time (interval between consecutive pulses).[35]

The spin−lattice relaxation time, $T_1$, represents the time required for the longitudinal component of the magnetization to recover its equilibrium value after the application of the perturbing pulse sequence. It is a measure of the dipolar interactions of the investigated spins with their surrounding. Its value ranges from tens to thousands of milliseconds for protons in hydrogenated compounds, and usually becomes smaller at lower temperatures.

$T_1$ relaxation times were obtained via the standard inversion recovery pulse sequence. In this pulse sequence, when the magnetization is in equilibrium and a $\pi$ pulse is applied, the magnetization tilts from the static field direction to its opposite (180°). Since no observable coherences are created, it still takes a further $\pi/2$ pulse to enable the measurement of $T_1$-relaxation. The $\pi/2$ pulse has the property to convert the population differences into observable coherences, tilting the magnetization by 90° into the plane orthogonal to the field direction.[35] In the applied sequence the delay between the $\pi$ and $\pi/2$ pulses is varied (35 delay times ranging from $10^{-5}$ to 45 s) in order to sample the longitudinal equilibrium recovery characterized by

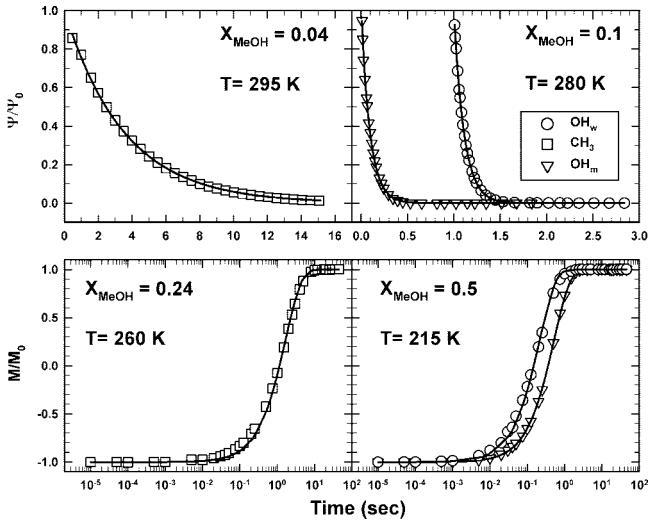


**Figure 1.** Examples of the fit performed for the calculation of the spin−spin relaxation, $T_2$, and spin−lattice relaxation, $T_1$, for four different molar fractions at four different temperatures in four panels each time showing either the methyl or the hydroxyl group data ($OH_w$, open circle; $OH_m$, open triangle; $CH_3$, open square). The data points are fitted according to the equations reported in the text and result in $T_2 = 2.55$ s for the $CH_3$ protons at 295 K in $X = 0.04$ (top left panel) and $T_2 = 0.09$ s and $T_2 = 0.11$ s for the $OH_m$ and $OH_w$ protons at 280 K in $X = 0.1$ respectively (top right panel). Note that the $OH_w$ $T_2$ data points (top right panel) are shifted by 1 s for visual reasons only. The fitted $T_1$ data yield $T_1 = 1.79$ s for the $CH_3$ protons at 260 K in $X = 0.24$ (bottom left panel) and $T_1 = 0.52$ s and $T_1 = 0.26$ s for the $OH_m$ and $OH_w$ protons at 215 K in $X = 0.5$ respectively (bottom right panel).

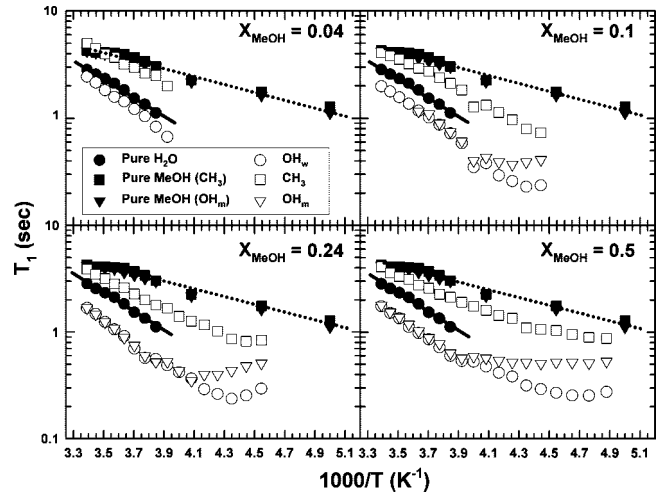


**Figure 2.** Spin−lattice relaxation times, $T_1$, as a function of temperature. Each panel reports $T_1$ of the protons for all functional groups ($OH_w$, open circle; $OH_m$, open triangle; $CH_3$, open square) in solution at a fixed methanol molar fraction and those for the pure liquids ($OH_w$, full circle; $OH_m$, full triangle; $CH_3$, full square). The Arrhenius slopes for the pure liquids are also reported as a reference for the reader (methanol, dotted line; water, solid line).

the $T_1$ relaxation time (Figure 1, bottom panels). The repetition time was set to 20 s and the number of scans was 16 for each delay time.

An insight into the dipolar interactions between spins belonging to the same species (i.e., an estimation of the strength of interplay among the same species) can be obtained by measuring the spin−spin relaxation times, $T_2$. A weaker interaction corresponds to a longer $T_2$. $T_2$ is the time required for the transverse component of the magnetization to vanish from the plane orthogonal to the static field direction.[35] In fact, when the magnetization is completely tilted in the plane orthogonal to the static field direction, a maximum phase coherence among the spins is created which will disappear spontaneously in a characteristic time, known as the apparent spin−spin relaxation time.

$T_2$ values were obtained by means of the Carr−Purcell−Meiboom−Gill pulse sequence.[36] Here a $\pi/2$ pulse is first applied to the spin system, then, after a variable time delay, a $\pi$ pulse is applied. This pulse rotates the magnetization by 180° about a direction orthogonal to the static field, causing the magnetization to rephase, at least partially, and produces a signal called echo. By varying the so-called echo time (TE), i.e. the time between the $\pi/2$ pulse and the maximum amplitude of the echo ($\Psi_0$), it is possible to evaluate the spin−spin relaxation time $T_2$. Thirty different echo times ranging from $10^{-2}$ to 6 s, for $OH_w$ and $OH_m$, and from 0.5 to 16 s for $CH_3$ were used (Figure 1, upper panels). The repetition time was set to 20 s and the number of scans was 16 for each TE.

All the experimental data were fitted by a single exponential law to extract the respective relaxation time as shown in Figure 1. In particular, the equation describing the equilibrium recovery of the longitudinal component of the magnetization is $M/M_0 = 1 - 2\exp(-\tau/T_1)$, where $M_0$ is the equilibrium value of the magnetization and $\tau$ is the delay time between the application of the two pulses. On the other hand, the equation describing the vanishing of the transversal component of the magnetization is given by $\Psi/\Psi_0 = \exp(-TE/T_2)$.[35]

Upon displaying both $1/T_1$ and $1/T_2$ on an Arrhenius plot, we were able to calculate the activation energies ($E_a$) for each functional group in different temperature ranges.

## Results and Discussions

The measured spin−lattice relaxation times for protons of the three functional groups in the water/methanol mixtures ($OH_w$, $OH_m$, and $CH_3$) are reported in Figure 2 as a function of temperature. Herein, in each panel the $T_1$ thermal behavior of the functional groups for one mixture at a given concentration together with that of the pure liquids is shown in a log−lin plot.

An inspection of Figure 2 shows that the spin−lattice relaxation times of the mixture components are shorter than those of the corresponding pure liquids, due to a strong interaction among them when mixed. This effect is more pronounced for the $OH_m$ group that is more strongly affected by the presence of water molecules. In addition, it is important to highlight that $T_1$ of both $OH_w$ and $OH_m$ take on, within the experimental error, the same value upon cooling until $T_k \cong 245$ K, temperature below which the two $T_1$ thermal behaviors split and flatten. Hence the two functional groups have the same chemical environment only for temperatures above $T_k$. This is true for all concentrations, even if for the concentration $X = 0.04$, at all $T$, and for $X = 0.1$, above 275 K, the resonance peaks of $OH_w$ and $OH_m$ coalesce into a single peak because of fast proton exchange.

Concerning the $T_1$ relaxation times of the $CH_3$ group, they are longer than those of the corresponding $OH_m$ and close to those of pure methanol over the entire investigated temperature range.

In the high temperature region the calculated activation energies, $E_a$, are found to be independent of the methanol molar fraction. and have a value of about 4.6 kcal/mol for the OH groups and 2.7 kcal/mol for the $CH_3$ group. The former value is equal to that of pure water, thus corresponds to hydrogen

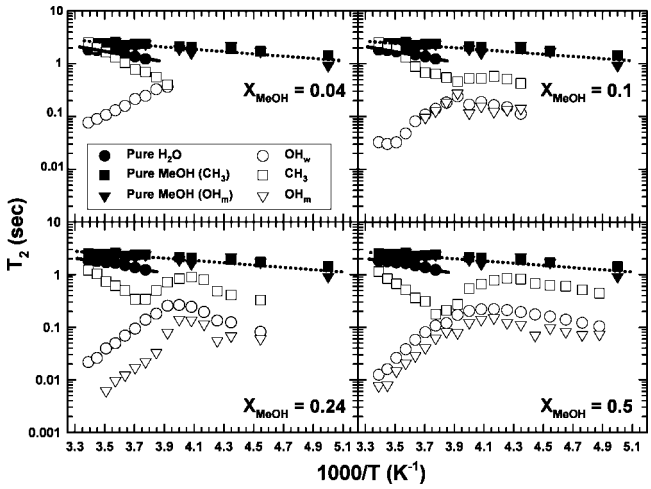


**Figure 3.** Spin−spin relaxation times, $T_2$, as a function of temperature. Each panel reports $T_2$ of the protons for all functional groups ($OH_w$, open circle; $OH_m$, open triangle; $CH_3$, open square) in solution at a fixed methanol molar fraction and those for the pure liquids ($OH_w$, full circle; $OH_m$, full triangle; $CH_3$, full square). The Arrhenius slopes for the pure liquids are also reported as a reference for the reader (methanol, dotted line; water, solid line).

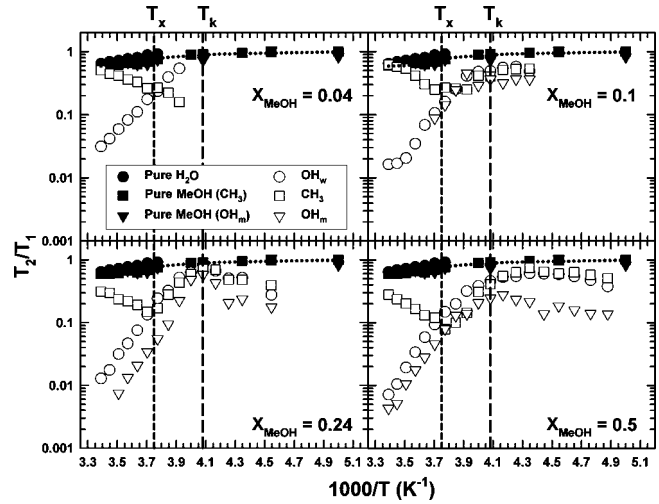


**Figure 4.** $T_2/T_1$ ratio as a function of temperature. Each panel reports $T_2/T_1$ of the protons for all functional groups ($OH_w$, open circle; $OH_m$, open triangle; $CH_3$, open square) in solution at a fixed methanol molar fraction and those for the pure liquids ($OH_w$, full circle; $OH_m$, full triangle; $CH_3$, full square). The temperatures $T_x$ and $T_k$ are indicated as a short-dashed line and a long-dashed line respectively. A guide for the eye is also drawn for the pure liquids (dotted line).

bonding activation energies, whereas the latter differs slightly from that of pure methanol (about 1 kcal/mol).

Figure 3 reports the thermal behavior of the spin−spin relaxation times of the mixtures at different concentrations and those of the pure liquids in a log-lin plot. Below $T_k \cong 245$ K, $T_2$ of each functional group behaves similarly to its corresponding relaxation time in the pure liquids. Indeed, below this temperature, $E_a$ of $OH_w$ and $OH_m$ in solution takes on a value of about 2.3 kcal/mol, which is very close to that of bulk water (about 2.1 kcal/mol).

Above $T_k$, it is interesting to notice an unusual thermal behavior of $T_2$ for the three functional groups in solution. In this thermal region, the experimental values of the spin−spin relaxation times of both $OH_w$ and $OH_m$ protons, for all concentrations, increase with decreasing temperature, in contrast to their shortening in the case of pure compounds. In addition, $T_2$ of the $CH_3$ protons in solution decreases sharply until about $T_x = 265$ K with a corresponding activation energy of about 7 kcal/mol, after which its thermal behavior starts to resemble those of the hydroxyl groups.

As stressed above, since $T_2$ is a measure of the interaction strength among the same functional groups, the lowering of $T_2$ for the hydroxyl groups, at ambient temperature, by about 2 orders of magnitude with respect to pure water and methanol (Figure 3) confirms that a strong hydrophilic interaction takes place. This, together with the coincidence in $T_1$ of $OH_m$ and $OH_w$, suggests that in solution the transient structures with the longest lifetime are hydrogen-bonded water/methanol aggregates, in agreement with the observation that the HB lifetime between $OH_m$ and $OH_w$ in solution is longer than that between the same species.[29,37]

Since $T_1$ contains information about both translational and rotational motions of the observed molecules and $T_2$ gives almost exclusively information on their rotation, the $T_2/T_1$ ratio is a dimensionless measure of the tumbling dynamics of the observed functional groups.[38] The $T_2/T_1$ ratio of all the functional groups in solution is smaller than that of pure liquids, implying a slowdown of the dynamics of the system. In addition, it shows a temperature behavior completely different from that of pure liquids (Figure 4). In more detail, the ratio for $OH_m$ and $OH_w$ increases sharply reaching a maximum value at about $T_k$, then it decreases more slowly upon further cooling. With reference to the $CH_3$ group, $T_2/T_1$ decreases with decreasing temperature until $T_x = 265$ K, where it overlaps with the $OH_w$ $T_2/T_1$ ratio, after which its thermal behavior resembles those of the hydroxyl groups.

The observed slowdown of the tumbling dynamics of all the functional groups, including the methyl one, is due to the formation of long-lived HBs among all the hydroxyl groups in solution. However, one must observe that the change in the $T_2/T_1$ values encloses a range of about 2 orders of magnitude for both $OH_m$ and $OH_w$ in the water/methanol mixtures, whereas the $T_2/T_1$ ratio values of the $CH_3$ protons only cover a range of about 1 order of magnitude. This means that the latter do not diverge much from the bulk methanol $T_2/T_1$ values, so its dynamics is not very much affected by the presence of water molecules in solution.

In order to explain the temperature dependence of the observed relaxation times it is necessary to understand if there are any and which are the structuring effects present in the solutions.[27] The physical properties of the water/methanol solution are intuitively determined by the interplay between the hydrophobic and hydrophilic moieties present in the mixture,[28] which generally depends on both concentration and temperature. The observed relaxation times suggest that, at ambient temperature, the hydrophilic effect encourages HB formation between water and methanol hydroxyl groups, which, as reported in literature, have a greater lifetime with respect to water−water and methanol-methanol HBs.[37] This longer HB lifetime is the cause of the creation of stable water−methanol clusters, reflecting a relatively good miscibility.[21] However, upon cooling, a segregation of methanol and water is favored, with a gradual development of single-component aggregates.[24] Thus, with decreasing temperature, a reorganization of HB clusters takes place from the mixed water/methanol at high temperature to the single species clusters at low temperature. This conclusion is mainly supported by the thermal behavior of $T_1$ of $OH_m$ and $OH_w$ for all the concentrations (Figure 2); in fact, as already mentioned, above $T_k$ the $T_1$ values at each temperature are coincident, indicating that $OH_m$ and $OH_w$ are bonded together

in the same lattice, whereas below $T_k$ $OH_m$ and $OH_w$ bond only with hydroxyls of the same species. A further evidence of the strong hydrophilic interaction is given by the very short $T_2$ of $OH_m$ and $OH_w$ (Figure 3). This quantity increases with decreasing temperature until $T_k$, signaling a reduced interaction between the hydroxyl groups thus the breaking of the mixed cluster. The dynamics of this HB rearrangement is partly influenced by the hydrophobic effect: while a cluster is breaking, the methyl groups have the possibility to interact with each other, causing their $T_2$ to decrease rapidly with decreasing temperature for $T > 265$ K. Below $T_x = 265$ K there is a small increase in the $T_2$ of the methyl group, since they interact less due to the formation of a new HB network. At $T_k \cong 245$ K, the $T_2$ of all functional groups in solution reaches a maximum and below this temperature it resembles that of the corresponding pure liquids. Therefore, below $T_k$ the water molecules develop random tetrahedral networks and methanol molecules organize themselves in rings and chains, as they do when not mixed.[39,40]

The HB reorganization is also reflected by the observed changes with temperature in the tumbling dynamics of the different functional groups in solution. The $T_2/T_1$ ratio of the $CH_3$ group decreases until $T_x \cong 265$ K (Figure 4), which confirms an increase in the interactions among the hydrophobic groups in the solution. Contrarily, $T_2/T_1$ of both $OH_m$ and $OH_w$ increases with cooling down until $T_k$ (Figure 4) and this indicates a diminishing hydrophilic interaction between the hydroxyl groups. Below $T_k$, the dynamics of the entire system slows down weakly.

When water is mixed with methanol, even at low methanol concentrations, its physical properties are obviously influenced by the interactions with this amphiphilic molecule. Such interactions are stronger at high temperatures due to the high stability of the mixed water/methanol HB clusters. However, upon cooling, an enhanced segregation of the system takes place and clusters of single species can form as evidenced by Dougan et al..[24] The driving mechanism behind the thermodynamic evolution of these systems is the hydrophilic interaction among hydroxyls, partially concurring with the hydrophobic interaction among methyls to determine an overall complex HB dynamics.

As all the reported results suggest, the key temperature in the thermal evolution of the HB dynamics is indeed $T_k \cong 245$ K, temperature at which both $T_1$ and $T_2$ of the functional groups in solution show special behaviors: spin−spin relaxation times have a maximum, while $OH_m$ and $OH_w$ spin−lattice relaxation times separate upon cooling. We want to stress that the latter evidence implies that the hydroxyl groups no longer interact with each other as they did above $T_k$ and prefer to organize themselves into aggregates of the same species. It is noteworthy that, for liquid water, the $T_k$ value is close to the temperature location of the Widom Line ($T_{WL}$). At this temperature the LDL structure of water becomes dominant over the HDL one, when dynamical heterogeneities develop within the system.[9] In other words, even in solution, upon reaching $T_k \equiv T_{WL}$ the water molecules prefer to bond with each other in order to develop their LDL network.

In conclusion, these $^1$H NMR relaxation studies point out that the thermodynamic properties of water/methanol solutions are governed by the HB dynamics, to some extent influenced by interactions among the hydrophobic methyl groups. HBs are continuously broken and formed between hydroxyl groups in solution; their lifetime and stability depend on both concentration and temperature. However, a similar trend in temperature of the measured relaxation times of each functional group at every concentration is observed and shows peculiar features at a common key temperature, $T_k = 245$ K. The interpretation of the results is consistent with the picture that above $T_k$ HB formation occurs among the different hydroxyl groups in solution, giving rise to local water/methanol clusters, whereas below this temperature HBs are preferably formed among hydroxyl groups of the same species.

These results may give an insight of what would happen in the case of large amphiphilic aqueous systems such as hydrated proteins, in which the hydration water could start to bond with the hydrophilic groups upon heating just at the Widom Line, letting proteins become biologically active.

**Acknowledgment.** The research at MIT is supported by the Materials Science Division of the US DOE. The research at Messina is supported by the MURST-PRIN2004. We benefited from affiliation with the EU Marie Curie Research and Training Network on Arrested Matter (Contract No. MRT-CT2003-504712); in particular, J.S. and C.K. are supported by research fellowships thereof. H.E.S. is supported by NSF Chemistry Grant CHE0616489.

## References and Notes

(1) (a) Debenedetti, P. G. *Metastable Liquids Concepts and Principles*; Princeton University Press, Princeton, NJ, 1996. (b) Kell, G. S. *J. Chem. Eng. Data* **1975**, *20*, 97. (c) Johari, G. P.; Hallbrucker, A.; Mayer, E. *Science* **1996**, *273*, 90.

(2) (a) Sastry, S.; Debenedetti, P. G.; Sciortino, F.; Stanley, H. E. *Phys. Rev. E* **1996**, *53*, 6144. (b) Rebelo, L. P. N.; Debenedetti, P. G.; Sastry, S. *J. Chem. Phys.* **1998**, *109*, 626.

(3) Poole, P. H.; Sciortino, F.; Essmann, U.; Stanley, H. E. *Nature* **1992**, *360*, 324.

(4) Xu, L.; Kumar, P.; Buldyrev, S. V.; Chen, S.-H.; Poole, P. H.; Sciortino, F.; Stanley, H. E. *Proc. Natl. Acad. Sci. U.S.A.* **2005**, *102*, 16558.

(5) Harrington, S.; Zhang, R.; Poole, P. H.; Sciortino, F.; Stanley, H. E. *Phys. Rev. Lett.* **1997**, *78*, 2409.

(6) Yamada, M.; Mossa, S.; Stanley, H. E.; Sciortino, F. *Phys. Rev. Lett.* **2000**, *88*, 195701.

(7) Mishima, O.; Stanley, H. E. *Nature* **1998**, *392*, 164.

(8) Liu, L.; Chen, S.-H.; Faraone, A.; Yen, C. W.; Mou, C.-Y. *Phys. Rev. Lett.* **2005**, *95*, 117802.

(9) Chen, S.-H.; Mallamace, F.; Mou, C.-Y.; Broccio, M.; Corsaro, C.; Faraone, A.; Liu, L. *Proc. Natl. Acad. Sci. U.S.A.* **2006**, *103*, 12974.

(10) Mallamace, F.; Branca, C.; Broccio, M.; Corsaro, C.; Mou, C.-Y.; Chen, S.-H. *Proc. Natl. Acad. Sci. U.S.A.* **2007**, *104*, 18387.

(11) Mallamace, F.; Broccio, M.; Corsaro, C.; Faraone, A.; Majolino, D.; Venuti, V.; Liu, L.; Mou, C.-Y.; Chen, S.-H. *Proc. Natl. Acad. Sci. U.S.A.* **2007**, *104*, 424.

(12) Mallamace, F.; Broccio, M.; Corsaro, C.; Faraone, A.; Wanderlingh, U.; Liu, L.; Mou, C.-Y.; Chen, S.-H. *J. Chem. Phys.* **2006**, *124*, 161102.

(13) (a) Mallamace, F.; Chen, S.-H.; Broccio, M.; Corsaro, C.; Crupi, V.; Majolino, D.; Venuti, V.; Baglioni, P.; Fratini, E.; Vannucci, C.; Stanley, H. E. *J. Chem. Phys.* **2007**, *127*, 045104. (b) Chen, S.-H.; Liu, L.; Fratini, E.; Baglioni, P.; Faraone, A.; Mamontov, E. *Proc. Natl. Acad. Sci. U.S.A.* **2006**, *103*, 9012.

(14) Kumar, P.; Yan, Z.; Xu, L.; Mazza, M. G.; Buldyrev, S. V.; Chen, S.-H.; Sastry, S.; Stanley, H. E. *Phys. Rev. Lett.* **2006**, *97*, 177802.

(15) Palo, D. R.; Dagle, R. A.; Holladay, J. D. *Chem. Rev.* **2007**, *107*, 3992.

(16) Derlacki, Z. J.; Easteal, A. J.; Edge, A. V. J.; Woolf, L. A.; Roksandic, Z. *J. Phys. Chem.* **1985**, *89*, 5318.

(17) Soper, A. K.; Dougan, L.; Crain, J.; Finney, J. L. *J. Phys. Chem. B* **2006**, *110*, 3472.

(18) Mikhail, S. Z.; Kimel, W. R. *J. Chem. Eng. Data* **1961**, *64*, 533.

(19) Frank, H. S.; Evans, M. W. *J. Chem. Phys.* **1945**, *13*, 507.

(20) Kauzmann, W. *Adv. Protein Chem.* **1959**, *14*, 1.

(21) Dougan, L.; Bates, S. P.; Hargreaves, R.; Fox, J. P.; Crain, J.; Finney, J. L.; Reat, V.; Soper, A. K. *J. Chem. Phys.* **2004**, *121*, 6456.

(22) Soper, A. K.; Finney, J. L. *Phys. Rev. Lett.* **1993**, *71*, 4346.

(23) Dixit, S.; Crain, J.; Poon, W. C. K.; Finney, J. L.; Soper, A. K. *Nature* **2002**, *416*, 829.

(24) Dougan, L.; Hargreaves, R.; Bates, S. P.; Finney, J. L.; Reat, V.; Soper, A. K.; Crain, J. *J. Chem. Phys.* **2005**, *122*, 174514.

(25) Laaksonen, A.; Kusalik, P. G.; Svishchev, I. M. *J. Phys. Chem. A* **1997**, *101*, 5910.

(26) Allison, S. K.; Fox, J. P.; Hargreaves, R.; Bates, S. P. *Phys. Rev. B* **2005**, *71*, 024201.
(27) Koga, Y.; Nishikawa, K.; Westh, P. *J. Phys. Chem. A* **2004**, *108*, 3873.
(28) Okazaki, S.; Touhara, H.; Nakanishi, K. *J. Chem. Phys.* **1984**, *81*, 890.
(29) Micali, N.; Trusso, S.; Vasi, C.; Blaudez, D.; Mallamace, F. *Phys. Rev. E* **1996**, *54*, 1720.
(30) Simpson, J. H.; Carr, H. Y. *Phys. Rev.* **1958**, *111*, 1201.
(31) Smith, D. W. G.; Powles, J. G. *Mol. Phys.* **1966**, *10*, 451.
(32) Krynicki, K.; Powles, J. G. *Proc. Phys. Soc.* **1964**, *83*, 983.
(33) Asahi, N.; Nakamura, Y. *J. Chem. Phys.* **1998**, *109*, 9879.
(34) Murthy, S. S. N. *J. Phys. Chem. A* **1999**, *103*, 7927.
(35) Abragam, A. *The Principles of Nuclear Magnetism*; Oxford: Oxford, U.K., 1961.
(36) (a) Carr, H. Y.; Purcell, E. M. *Phys. Rev.* **1954**, *94*, 630. (b) Meiboom, S.; Gill, D. *Rev. Sci. Instrum.* **1958**, *29*, 688.
(37) Ferrario, M.; Haughney, M.; McDonald, I. R.; Klein, M. L. *J. Chem. Phys.* **1990**, *93*, 5156.
(38) Stringfellow, T. C.; Farrar, T. C. *J. Phys. Chem.* **1995**, *99*, 3889.
(39) Asahi, N.; Nakamura, Y. *Chem. Phys. Lett.* **1998**, *290*, 63.
(40) Guo, J.-H.; Luo, Y.; Augustsson, A.; Kashtanov, S.; Rubensson, J. E.; Shuh, D. K.; Agren, H.; Nordgren, J. *Phys. Rev. Lett.* **2003**, *91*, 157401.

JP803456P